UV-driven hydroxyl radical oxidation of tris(2-chloroethyl) phosphate: Intermediate products and residual toxicity

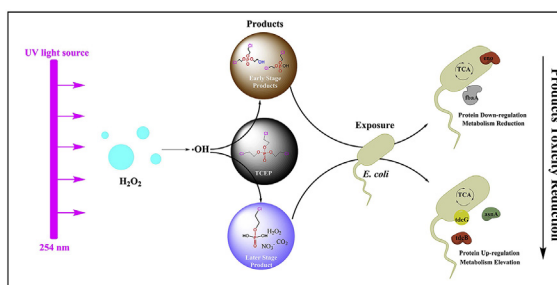Juan Liu [a], Jinshao Ye [a, b], Yifu Chen [a], Chongshu Li [a], Huase Ou [a, *]

[a] School of Environment, Guangzhou Key Laboratory of Environmental Exposure and Health, Guangdong Key Laboratory of Environmental Pollution and Health, Jinan University, Guangzhou 510632, China
[b] Joint Genome Institute, Lawrence Berkeley National Laboratory, Walnut Creek 94598, CA, USA

HIGHLIGHTS

- Degradation of TCEP by UV/H$_2$O$_2$ involves hydroxylation and dechlorination.
- Proteomics analysis is used to evaluated detoxification of TCEP.
- Incomplete degradation products of TCEP activates metabolism of *Escherichia coli*.
- Toxicity of incomplete degradation products is obviously weakened.

GRAPHICAL ABSTRACT

ABSTRACT

Organophosphorus esters (OPEs) are emerging contaminants widely applied as annexing agents in a variety of industrial products, and they are robust against conventional wastewater treatments. Ultraviolet-driven (UV) radical-based advanced oxidation processes have a potential to become cost-effective treatment technologies for the removal of OPEs in water matrix, but residual and newly generated toxicities of degradation products are a concern. This study is a comprehensive attempt to evaluate UV/H$_2$O$_2$ for the degradation of a water dissolved OPE, tris(2-chloroethyl) phosphate (TCEP). In ultrapure water, a pseudo-first order reaction was observed, and the degradation rate constant reached 0.155 min^{-1} for 3.5 μM TCEP using 7.0 mW cm^{-2} UV irradiation with 44.0 μM H$_2$O$_2$. Hydroxyl radicals were involved in the oxidative degradation of TCEP, as demonstrated by the quenching of the degradation reaction in the presences of tertiary butanol or ethanol. High resolution mass spectroscopy data showed a partial transformation of TCEP to a series of hydroxylated and dechlorinated products e.g., C$_4$H$_9$Cl$_2$O$_4$P, C$_6$H$_{13}$Cl$_2$O$_5$P and C$_2$H$_6$ClO$_4$P. Based on proteomics data at molecular and metabolic network levels, the toxicity of TCEP products was reduced obviously as the reaction proceeded, which was confirmed by the up-regulated tricarboxylic acid cycle, fatty acid metabolism and amino acid metabolism in *Escherichia coli* cells exposed to degradation products mixture. In conclusion, incomplete hydroxylation and dechlorination of TCEP likewise are effective for its detoxification, indicating that UV/H$_2$O$_2$ can be a promising treatment method for OPEs removal.

© 2017 Elsevier Ltd. All rights reserved.

1. Introduction

With the ban of polybrominated diphenyl ethers and

polychlorinated diphenyl ethers, organophosphate esters (OPEs) as their substitutes have been widely applied as annexing agents in a variety of industrial products, such as plastics, electronics, buildings and vehicles (Cristale et al., 2016). Organophosphate esters are used as flame retardants, plasticizers and heat insulation agents. However, the latest research has found that OPEs also have potential persistence, bioaccumulative capacity and toxicity (Kim et al., 2011; Ezechias et al., 2014; Guo et al., 2017). Numerous OPEs have been detected in fish as a result of bioaccumulation (Kim et al., 2011; Guo et al., 2017), and they can cause atopic dermatitis, asthma and even reduction of male sperm quality (Meeker and Stapleton, 2010; Araki et al., 2014). Therefore, OPEs are emerging environmental contaminants.

To date, OPEs have been detected in fresh water worldwide (Andresen et al., 2004). The concentrations of OPEs in rivers have been reported to reach several hundred ng L^{-1} (Zeng et al., 2015; Shi et al., 2016). Municipal and industrial effluents are two primary sources of OPEs for natural water bodies. Some studies have shown that OPEs cannot be effectively degraded in conventional biological treatment processes (Reemtsma et al., 2006; Martinez-Carballo et al., 2007), resulting in $\mu g\ L^{-1}$ OPE residuals in the secondary effluent of wastewater treatment plants (Meyer and Bester, 2004), especially the chlorinated OPEs (Zeng et al., 2015). Furthermore, OPEs have been detected even in finished drinking water (Stackelberg et al., 2004), implying that conventional drinking water treatment processes were ineffective for OPEs removal. Therefore, it is desirable to develop high efficiency and energy-saving treatment methods for OPEs control.

Numerous advanced oxidation processes (AOPs), including ozonation, photochemical oxidation, electrochemical oxidation and ultrasonic oxidation, were attempted for the elimination of organic contaminants (Meng et al., 2010). Ultraviolet-driven AOPs (UV-AOPs) e.g., UV/H$_2$O$_2$, UV/TiO$_2$, UV/persulfate and Fenton oxidation, show a great potential as low-cost and environmental-friendly technologies for persistent organic contaminants removal (Pillai et al., 2015). Dedicated research about the potential applications of UV-AOPs for OPEs elimination has only started so far. Yuan et al. (2015) have found that UV/H$_2$O$_2$ was more efficient than ozonation for the degradation of OPEs in a municipal secondary effluent. Ruan et al. (2013) have found that the degradation of OPEs by UV/H$_2$O$_2$ followed pseudo-first-order kinetics, and a portion of their degradation products could become available carbon sources for bacterial growth after UV/H$_2$O$_2$ treatment (Watts and Linden, 2008). However, there is still a knowledge gap on the detailed mechanisms and pathways involving the degradation of OPEs using UV-AOPs, not to mention the environmental safety of their degradation products.

A full mineralization of the targeted organic contaminants will consume a lot of energy and chemical materials in actual UV-AOPs for water treatment. Other coexisting contaminants e.g., particulate matter, inorganic ions, natural organic matter and other persistent organic pollutants, may become potential competitors to consume ·OH (Dodd et al., 2009). Incomplete degradation of targeted contaminants (e.g., OPEs) will be common in UV-AOPs applications. Therefore, a comprehensive toxicological assessment of OPEs and their degradation products is essential. Interactions between OPEs (or their products) and organisms involve a series of molecular mechanisms of action within fundamental physiological processes; and related exploration of protein expressions and metabolic pathways will reveal unknown negative effects of OPEs on organisms and newly generated toxicity of degradation products. So far, the existing toxicological evaluation of OPEs has been limited to traditional techniques, such as zebrafish test (Kim et al., 2015), water flea test (Waaijers et al., 2013) and cell line test (Ta et al., 2014).

This study was designed to explore the degradation efficiency and mechanism of a water dissolved OPE, tris(2-chloroethyl) phosphate (TCEP), with 254 nm UV/H$_2$O$_2$ oxidation. High resolution mass spectrometry (HRMS) was used to determine the degradation products of TCEP, followed by the speculation of degradation pathways. The biological effects of degradation products on fundamental protein expressions and metabolic networks were evaluated with a quantitative proteomic technology using *Escherichia coli* as a model organism.

2. Materials and methods

2.1. Materials

Tris (2-chloroethyl) phosphate (99%, HPLC grade) and tris(2-chloro-1-methylethyl) phosphate (99%, HPLC grade) were purchased from Toronto Research Chemicals (CAN). Humic acid (HA) (90% dissolved organic matter, CAS: 1415-93-6), tertiary butanol (98%), ethyl alcohol (98%) and isobaric tags for relative and absolute quantitation (iTRAQ) reagent multiplex kit (PN 4352135) were purchased from Sigma-Aldrich (USA). Analytical grade H$_2$O$_2$ (30%, v/v), NaNO$_3$ (98%) and NaCl (98%) were purchased from Sinopharm (China). *Escherichia coli* ATCC11303 used in the current experiments was a standard strain purchased from the microbial culture collection center in Guangdong Province, China. Chemical reagents were prepared using the highest purity available (Table S1 of the Supporting Information; "S" designates texts, tables, figures and other contents in the Supporting Information thereafter). All reagents were stored at 4 °C or −20 °C as required. All of the solutions were prepared using ultrapure water (18.2 MΩ) produced by a Milli-Q Advantage A10 system (Millipore, USA). *E. coli* was stored at −80 °C with glycerin before used.

2.2. UV irradiation module and degradation experiments

The UV irradiation device was composed of the following modules: power source, UV light source, irradiation shield, heat sink and reactor vessel (Fig. S1). The device frame was drawn using AutoCAD, and then was produced by a 3D printing instrument. The UV light source was a low-pressure mercury lamp (power 8 W, effective length 24 cm, Philips, Holland) with a maximum emission peak at 254 nm; the irradiation intensity was measured by a HAAS-3000 light spectrum irradiation meter (Everfine, China). In the UV/H$_2$O$_2$ experiments, the irradiation intensity on the surface of the solution was adjusted to 7.0 mW cm^{-2}. The reaction vessel was a circular quartz vessel with a diameter of 12 cm.

A stock solution of TCEP at 100.0 mg L^{-1} was prepared. Initial concentration of TCEP was varied from 0.1 mg L^{-1} to 10.0 mg L^{-1} (0.35−35.00 μM). The initial concentration of H$_2$O$_2$ was in the range of 0.15−7.48 mg L^{-1} (4.4−220.0 μM). Reaction conditions were maintained at 25 ± 2 °C, pH = 6.8−7.2, and the reaction solution was orbitally shaken at 60 rpm. Solution pH was adjusted by pH buffered solution, which contained different concentration values of NaOH, KH$_2$PO$_4$ and H$_3$PO$_4$. For example, the buffered solution at pH = 6.85 contains 50 mmol KH$_2$PO$_4$ and 23.6 mmol NaOH. For HA experiments, a stock solution at 1 g L^{-1} was prepared by adding HA into ultrapure water and filtering with 0.22 μm polyethersulfone filter. The concentrations of both NaNO$_3$ and HA were varied between 1 and 100 mg L^{-1}. At a pre-defined time, 20 mL of the sample was withdrawn and filtrated by a 0.22 μm polyether sulfone filter, and then it was transferred into a brown amber tube at 4 °C before analysis.

Second-order rate constants for the reaction of TCEP (*T*) with ·OH was determined by competition kinetics in a binary mixture

with *para*-chlorobenzoic acid (pCBA) as a reference compound (*R*) (Keen and Linden, 2013). Using the ·OH reaction rate constant with the reference compounds (k_R), the ·OH reaction rate constant with TCEP (k_T) was determined according to eq. (1) (Huber et al., 2003).

$$\ln\left(\frac{[T]}{[T]_0}\right) = \frac{k_T}{k_R}\left(\frac{[R]}{[R]_0}\right) \tag{1}$$

2.3. Ion and total organic carbon analyses

Concentrations of PO_4^{3-} and Cl^- were determined by an ICS - 2500 analyzer (Dionex, USA). The mobile phase of DIONEX IonPac AS15 column was 30.0 mM NaOH solution. Total organic carbon (TOC) was determined by a liquid TOC-trace analyzer (Elementar, Germany).

2.4. Quantitative analysis of tris(2-chloroethyl) phosphate and qualitative analysis of its intermediates

Quantitative analysis of TCEP was performed using a HPLC-MS/MS system with a TripleQuad 5500 tandem mass spectrometry (Applied Biosystems SCIEX, USA), while the determination of organic intermediate products was conducted using a time-of-flight HRMS (TripleTOF 5600+, Applied Biosystems SCIEX, USA). The detailed analysis procedure is presented in Text S1, Tables S2 and S3. The determination of generation product followed a systematic intermediate screening procedure presented in our previous study (Ou et al., 2017).
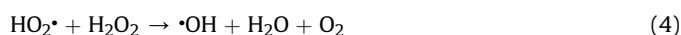
2.5. Proteomics analysis

Proteomics analysis included four stages: (1) exposure to targeted contaminants, (2) protein digestion, (3) iTRAQ labeling and (4) HRMS analysis. The targeted contaminant samples for proteomics analysis included: (1) 60 mL ultrapure water (control), (2) 60 mL of 3.5 μM TCEP solution, (3) 60 mL UV/H_2O_2 treated sample #1 (UV/H_2O_2 intermediate mixture #1; reaction time = 5 min), (4) 60 mL UV/H_2O_2 treated sample #2 (UV/H_2O_2 intermediate mixture #2; reaction time = 20 min). The reaction conditions were: temperature 25 ± 2 °C, pH 6.8–7.2, $[TCEP]_0$ = 3.5 μM, $[H_2O_2]_0$ = 44.0 μM. *Escherichia coli* ATCC11303 was selected as the model microorganism, which was inoculated at 100 rpm for 12 h. The *E. coli* cells were obtained by centrifugation at 3500*g* for 10 min and were washed three times. These cells (0.1 g L^{-1}) were inoculated into a 100 mL medium containing 30 mg L^{-1} KH_2PO_4, 70 mg L^{-1} NaCl, 30 mg L^{-1} NH_4Cl, 10 mg L^{-1} $MgSO_4$, 30 mg L^{-1} beef extract, 100 mg L^{-1} peptone. One milliliter of the 100.0 mg L^{-1} TCEP stock solution (or its intermediate mixture) was added to obtain a 1 mg L^{-1} final concentration, and then the bacteria suspension was cultivated in the dark at 25 °C on a rotary shaker at 100 rpm for 24 h. After exposure, the cells were separated and washed using phosphate buffer solution for protein extraction. The subsequent protein digestion, iTRAQ labeling and HRMS analysis followed the same procedure described in our previous research (Ou et al., 2017). Compared with the control samples, proteins in the cells after exposure to target pollutants with at least a 1.2-fold increase or decrease in concentration were identified as the up- or down-regulated expression proteins.

3. Results and discussion

3.1. Degradation kinetics and mineralization

Slight variations of TCEP were observed in the control experiments using water, H_2O_2 and UV experiments (Fig. 1a), suggesting that TCEP was stable in ultrapure water and H_2O_2 solution, and the 254 nm irradiation cannot induce direct photolysis of TCEP. The degradation efficiency of TCEP increased significantly when UV and H_2O_2 were combined. For 3.5 μM (1 mg L^{-1}) TCEP, the degradation efficiency increased to ~99% after 30-min 254 nm UV/H_2O_2 reaction (UV intensity at 7.0 mW cm^{-2}; $[H_2O_2]_0$ = 44.0 μM). Based on the fitting calculation, a pseudo-first order reaction was confirmed (Fig. 1b). The degradation rate constant (k_{obs}) reached 0.155 min^{-1} with a half-life of 4.5 min. This high degradation efficiency of TCEP may be attributed to the oxidative ·OH (oxidation potential at 2.8 V) generated by the UV-induced homolysis of H_2O_2 (Crittenden et al., 1999; Zhou and Smith, 2001; Shen and Wang, 2002):

$$H_2O_2 + h\nu \rightarrow 2\cdot OH \tag{2}$$

$$\cdot OH + H_2O_2 \rightarrow HO_2\cdot + H_2O \tag{3}$$

$$HO_2\cdot + H_2O_2 \rightarrow \cdot OH + H_2O + O_2 \tag{4}$$

$$2\cdot HO_2\cdot \rightarrow H_2O_2 + O_2 \tag{5}$$

$$HO_2\cdot + \cdot OH \rightarrow H_2O + O_2 \tag{6}$$

To confirm the existence of ·OH radicals, the scavengers tertiary butanol and ethyl alcohol were added. As shown in Fig. S2, only slight variations of TCEP were observed in the presence of tertiary butanol or ethyl alcohol, indicating that the radical-based oxidation was inhibited. In competition experiment using pCBA as the reference compound (Fig. S3), the second-order rate constants for TCEP with ·OH reached ~2.5 × 10^8 M^{-1} s^{-1}, which was obviously lower than pCBA (5.0 × 10^9 M^{-1} s^{-1}) (Huber et al., 2003).

Variation of TOC is presented in Fig. 1c, with an initial value of 2.96 mg L^{-1} at time zero. Approximately 60% TOC was removed after 60 min reaction, indicating that the mineralization of TCEP was incomplete. One TCEP molecule contains one central phosphorus backbone and three chlorine terminals, and they can be transformed to PO_4^{3-} and Cl^-, respectively. The concentrations of PO_4^{3-} and Cl^- increased from 0 to 2.35 mg L^{-1} and 3.68 mg L^{-1} after 60-min reaction (Fig. 1d), suggesting a gradual mineralization of TCEP. Theoretically, 3.5 μM TCEP can be mineralized into 3.33 mg L^{-1} PO_4^{3-} and 3.68 mg L^{-1} Cl^-. The result of Cl^- indicated that all chlorine terminals were degraded. In contrast, taking into account the results of PO_4^{3-} and TOC, the central phosphorus and ethyl side chains of TCEP still remained, implying that TCEP was transformed to a series of intermediates.

3.2. Influence factors

The concentration of H_2O_2 is an important influence factor in UV/H_2O_2 degradation experiments. In this study, when the H_2O_2 concentration increased from 4.4 μM to 44.0 μM, only a slight effect on the degradation efficiency was observed (Fig. S4). The reaction rate decreased obviously when the concentration of H_2O_2 increased to 220.0 μM. Since H_2O_2 is an important ·OH scavenger at high concentration (Crittenden et al., 1999), the excess H_2O_2 competed with TCEP for reaction with ·OH, which would reduce the degradation efficiency of TCEP.

Variation of pH is also a crucial factor for UV-AOPs reactions.

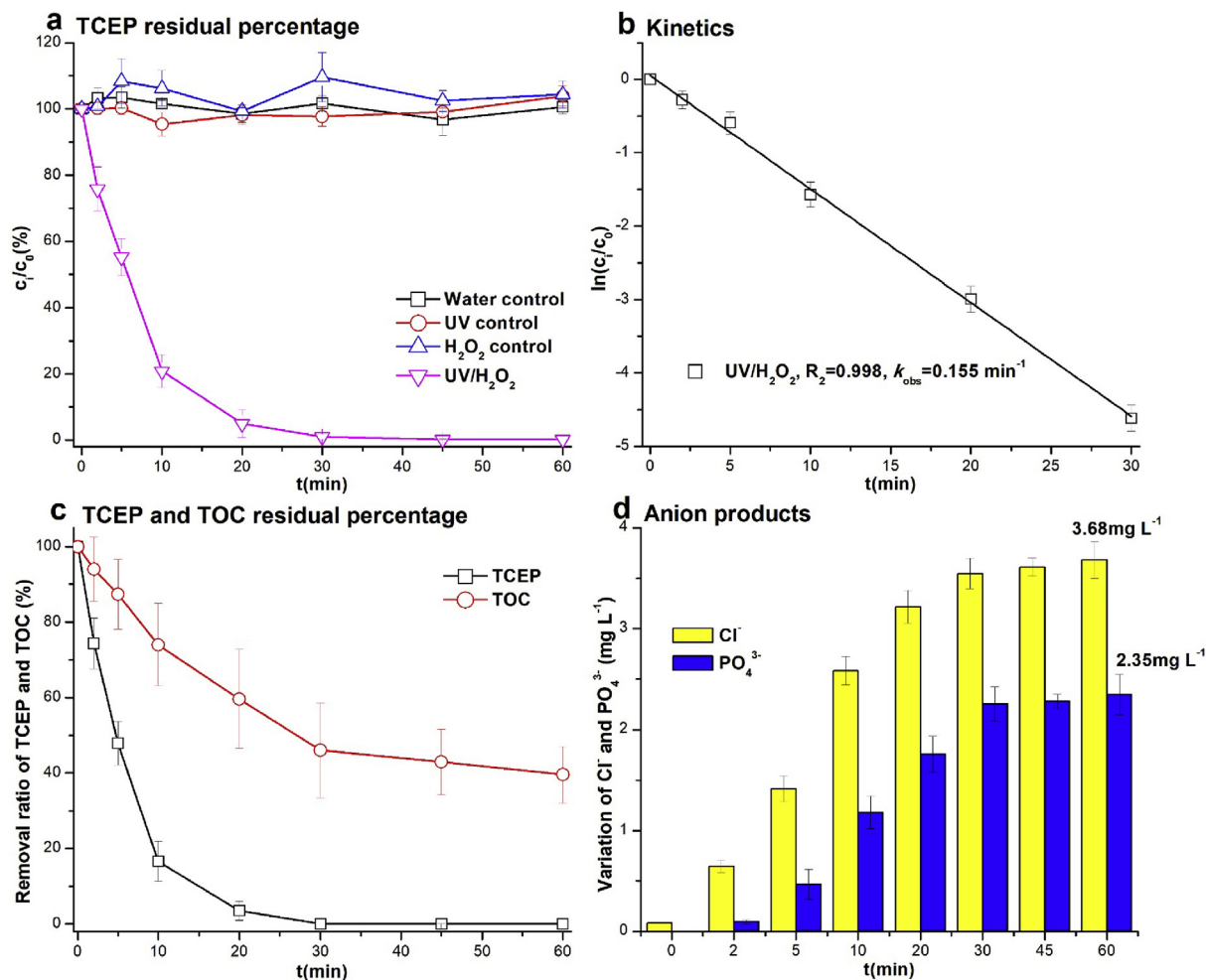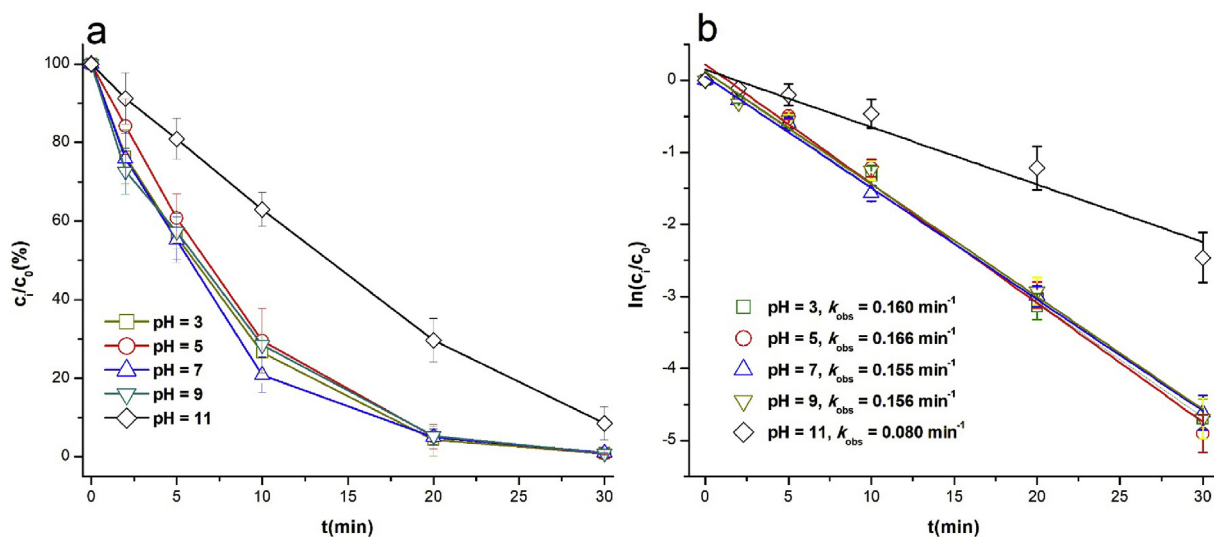**Fig. 1.** Degradation efficiency and mineralization of tris(2-chloroethyl) phosphate.

Fig. 2. Influence of different pH in UV/H_2O_2 experiments.

Results of TCEP degradation under different pH values are presented in Fig. 2. When pH increased from 3.0 to 9.0, k_{obs} retained in the range of 0.155–0.166 min^{-1}. Some studies have shown that pH

had a slight effect on the degradation efficiency of TCEP under acidic condition (Ghaly et al., 2001), which is consistent with our results. However, a severe inhibition was observed in this study

under alkaline condition. Since phosphate buffer solution was used in pH influence factor experiment, the effects of phosphates should be considered. The reaction rate between phosphates and ·OH was lower ($k_{\cdot OH}$ with $H_2PO_4^-$ at ~2.0×10^4 M^{-1} s^{-1}, $k_{\cdot OH}$ with HPO_4^{2-} at 1.5×10^5 M^{-1} s^{-1}) (Buxton, 1988) than that of TCEP with ·OH (~2.5×10^8 M^{-1} s^{-1}), but a high concentration of phosphates (for example, 50 mM phosphates at pH 6.85) was added, especially under alkaline condition (an increasing fraction of PO_4^{3-}). Therefore, the phosphates may also become ·OH scavengers, inhibiting the degradation of TCEP. It should be noted that an inhibition was observed at pH = 11.0 (k_{obs} was 0.080 min^{-1}). Furthermore, since pH 11 is close to the pK_a of H_2O_2 (eq. (8)) (Crittenden et al., 1999), the deprotonation of H_2O_2 induced the formation of HO_2^-, which is another competitive target for ·OH (eq. (8)). This reaction is actually over 100 times faster than reaction (eq. (3)) (Buxton, 1988), resulting in the inhibition of TCEP oxidation efficiency.

$$H_2O_2 \rightleftharpoons H^+ + HO_2^- (pK_a = 11.6) \tag{7}$$

$$HO_2^- + \cdot OH \rightarrow HO_2 \cdot + OH^- \tag{8}$$
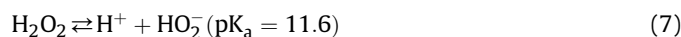
NO_3^- and HA are two common impurities in natural water bodies, and their influence on the TCEP degradation is shown in Fig. S5. When the concentration of HA increased from 0 to 100 mg L^{-1}, k_{obs} changed from 0.155 min^{-1} to 0.063 min^{-1}. It should be noted that, when HA increased from 0 to 5 mg L^{-1}, k_{obs} increased a little; when HA increased from 5 mg L^{-1} to 100 mg L^{-1}, k_{obs} obviously decreased. Under UV irradiation, low concentration HA may be transformed to some transient species, such as triplet states (Canonica et al., 1995), which improved the degradation of TCEP. High concentration HA had an inhibition on the TCEP degradation using UV/H_2O_2, which may be due to its absorption of UV irradiation, reducing the UV photon flux for TCEP degradation. The consumption of ·OH by HA further reduced the degradation efficiency of TCEP. Compared to HA, NO_3^- had a slight impact on the reaction, and k_{obs} retained in the range of 0.155—0.167 min^{-1} when NO_3^- concentration increased from 1 mg L^{-1} to 100 mg L^{-1}.

3.3. Degradation intermediates and generation pathways

Through the comparison of molecular weight, isotopic distribution and ion fragment obtained by the HRMS data (detailed procedure was discussed in Text S1), three stable products, including product A ($C_4H_9Cl_2O_4P$, m/z 222.97, 224.97), product B ($C_6H_{13}Cl_2O_5P$, m/z 266.99, 268.99) and product C ($C_2H_6ClO_5P$, m/z 160.98, 162.97), were confirmed. Detailed HRMS information concerning these products is presented in Figs. S5-S7, and their generation pathways were proposed (Fig. 3).

Product A (Fig. S6) has a MW of 222.99 Da, which was generated through the addition of a hydroxyl radical onto the phosphorus backbone, followed by breaking of an oxygen-ethyl-chloride arm chain. Product B (Fig. S7) has a MW of 267.04 Da. It was generated by substitution of a chlorine atom at the end of a branched chain, which was directly replaced by a hydroxyl group. Product C (Fig. S8) has a MW of 160.49 Da, and it was generated by the cleavage of another oxygen-ethyl-chloride chain following a similar process as product A.

Relative intensity variations of these products are presented in Table 1. The intensity is defined as the peak area of the targeted extracted ion flow in mass spectroscopy data. The intensity of product A increased to 1.5×10^6 at about 5 min. The time trend of product B was similar, and its intensity reached the maximum value (~4×10^5) at 2 min. Product C, which was proposed to be a further

oxidation product of product A, had a concentration maximum at 20 min. The product C at a later time suggested a generation order from product A to product C. After reaching the peak values, all the product intensities reduced to low levels after 45-min reaction, implying transformations to further unknown degradation products. It should be noted that product A was the intermediate product with the highest intensity.

3.4. Differential protein expressions and safety evaluation

Based on the time evolution of degradation products, the reaction times of samples for proteomics analysis were set at 5 min and 20 min. At 5 min, the abundances of product A and TCEP were relatively high. At 20 min, the abundances of all three products decreased to low levels, and the removal efficiency of TCEP reached 95%. Therefore, quantitative comparison (up-regulation or down-regulation) of the protein expression between *E. coli* cells exposed to TCEP (or its degradation intermediates) and healthy cells (control group) was attempted. For example, if a protein has a higher abundance (1.2-fold) in the *E. coli* cells exposed to TCEP compared to the cells exposed to ultrapure water (control), it is defined as an up-regulation protein.

Compared to healthy cells, *E. coli* cells exposed to 1 mg L^{-1} TCEP showed up-regulated expressions of proteins related to oxidative phosphorylation, as well as purine, glucose, glycine, glutamate, aspartate and fructose metabolisms. Some down-regulated metabolic pathways, including citrate cycle, pentose phosphate pathway, unsaturated fatty acid biosynthesis, as well as serine, L-aspartate, pyruvate, glutathione and biotin metabolisms, were also observed (Fig. S9). The alteration of these metabolic pathways confirmed that carbohydrate, lipid and biotin metabolisms were the main target pathways suppressed by TCEP. The increasing synthesis of nucleotides for DNA formation implied a DNA self-repair (Munoz et al., 2017). To offer glutamate, glycine, inorganic phosphate and other precursors for DNA synthesis, fatty acids and low-molecular-weight organic acids were consumed through the up-regulated fatty acid biodegradation pathway and the down-regulated citrate cycle (Kusnadi et al., 2015). Some phospholipids and non-essential polysaccharides, such as starch, glycan and dextrin, were accordingly down synthesized.

Exposure to 5-min UV/H_2O_2 degradation intermediate mixture induced alterations of further metabolic pathways. Compared to the change of metabolic network triggered by TCEP, the up-regulation of pentose phosphate pathway and amino acid biosynthesis confirmed that the toxicity of the intermediate mixture significantly decreased (Fig. S10). This finding further clarified that the central carbohydrate metabolism was the target pathway stressed by TCEP. Compared with the control samples, exposure to 20-min UV/H_2O_2 degradation intermediate mixture induced significant up regulation of citrate cycle and biotin metabolism, and it triggered the down-regulation of the metabolism of arachidonic acid (Fig. 4). After 20-min UV/H_2O_2 treatment, TCEP was transformed to a series of further degradation products. *Escherichia coli* cells exposed to this degradation intermediates mixture exhibited significant activations of critical metabolism pathways e.g., citrate cycle, fatty acid and amino acid metabolism (Fig. 4), suggesting that the intermediate products generated at 5 min UV/H_2O_2 treatment were further detoxified.

To further quantitatively depict the toxicity variation of TCEP and its intermediates mixture, 550 up-regulated and down-regulated proteins were selected (Table S4). Tris (2-chloroethyl) phosphate and its intermediates triggered opposite expression trends of these selected proteins (Fig S10). Especially, citrate cycle, pentose phosphate pathway and amino acid metabolism exhibited
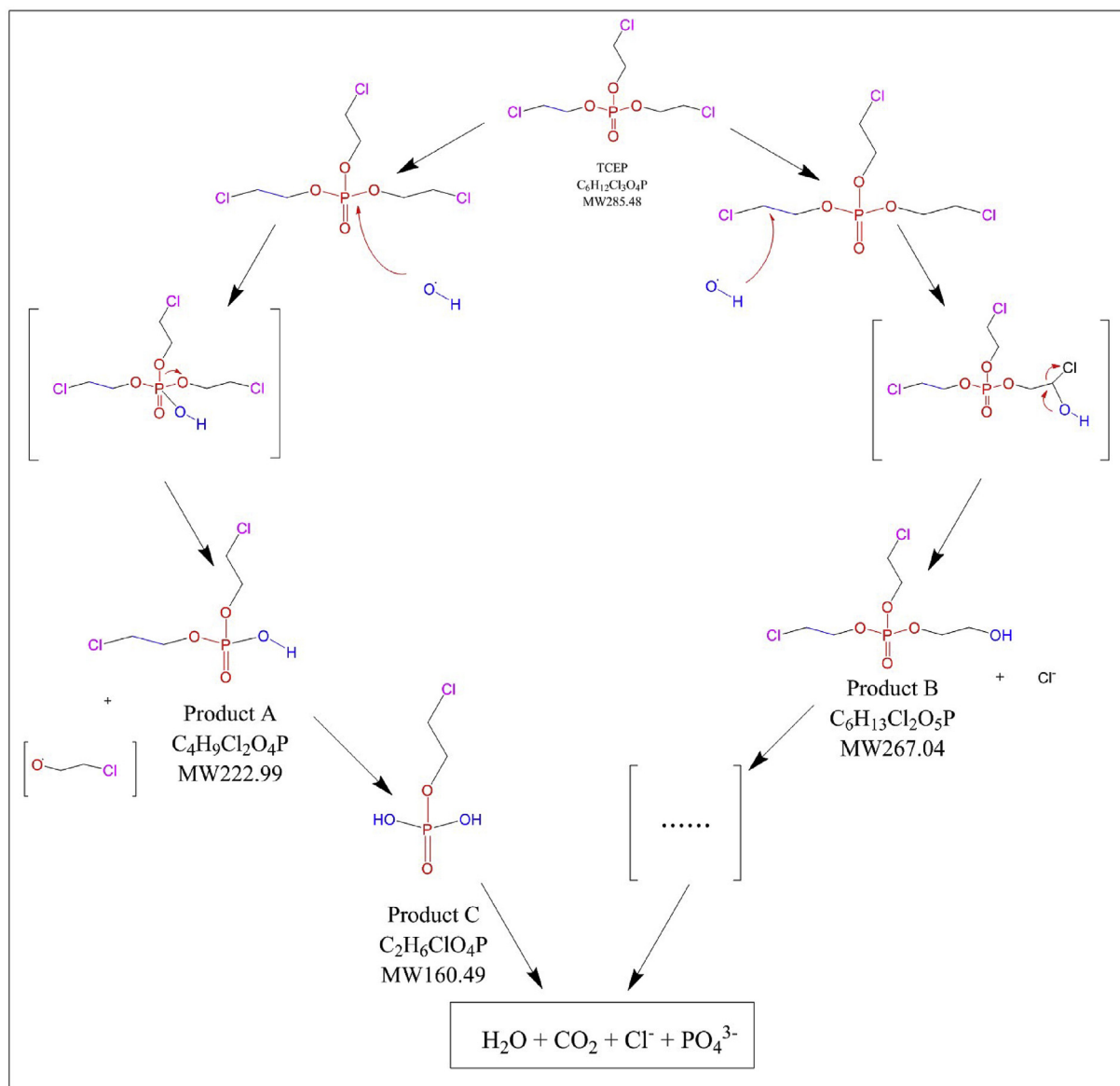
Fig. 3. Proposed generative pathways of degrading products from tris(2-chloroethyl) phosphate in 254 nm UV/H$_2$O$_2$ system.

opposite regulation trends in *E. coli* exposed to TCEP and 20-min UV/H$_2$O$_2$ degradation intermediate mixture. For amino acid metabolism, FbaB, GltA, HisA and LtaE showed the same up-regulated tendency, whereas, RpiA was down-expressed under the stresses of TCEP and its intermediates (Fig. 5), implying that these five proteins could be used as biomarkers to identify the occurrences of TCEP and its by-products in water matrix. Up-regulated expressions of AcnB, Asd, AsnA, DapA, GlyA, TdcB, TdcG, ThrB, TktA and TrpA under the stresses of TCEP intermediates revealed that these proteins could indicate the detoxification efficiency of TCEP.
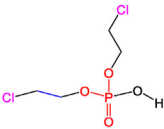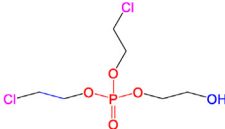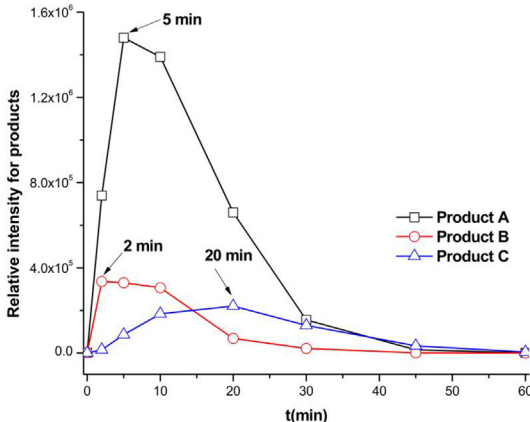
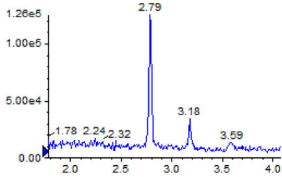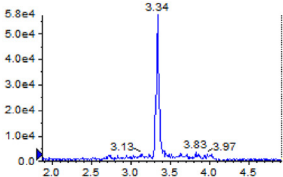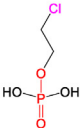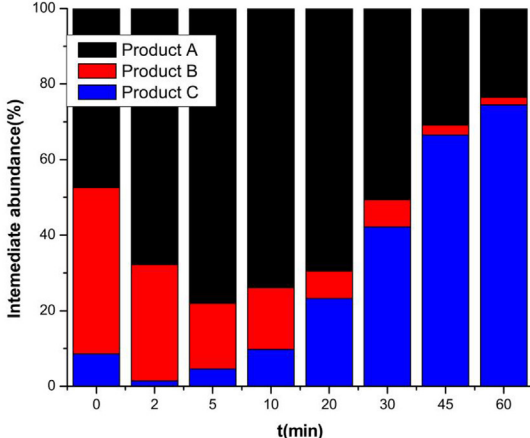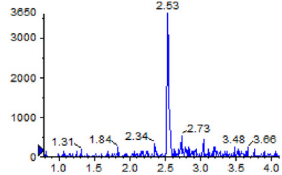### 3.5. Assessment of energy consumption

According to the above results, UV/H$_2$O$_2$ would be an efficient treatment method for TCEP removal and detoxification. The assessment of energy consumption can provide more information for its systematic evaluation. Electrical energy per order (EE/O)

analysis is a common tool to assess the electrical cost of UV-AOPs, and the EE/O is defined as the electrical energy (kilowatt per hour; kWh) required to degrade a target contaminant by one order of magnitude in 1 m^3 contaminated matrix. A detailed calculation procedure can be found in He et al. (2013):

$$EE/O = \frac{P \times t}{V \times \lg\left(c_i/c_f\right)}$$

(9)

where, EE/O has the unit of kWh m^{-3} order^{-1}; P represents the total electrical power to drive UV irradiation entering the matrix, kW; V is the volume of reaction matrix, m^3; c_i indicates the initial concentration of the target contaminant, mg L^{-1}; c_f indicates the final concentration of the target contaminant after reaction, mg L^{-1}, t indicates the time at which the concentration of target contaminant decreases from c_i to c_f, h. In the current study, the c_i/c_f was set at 10, and the t indicated the time 90% TCEP was removed.

Table 1

Tris (2-chloroethyl) phosphate organic intermediates in UV/H_2O_2 system.

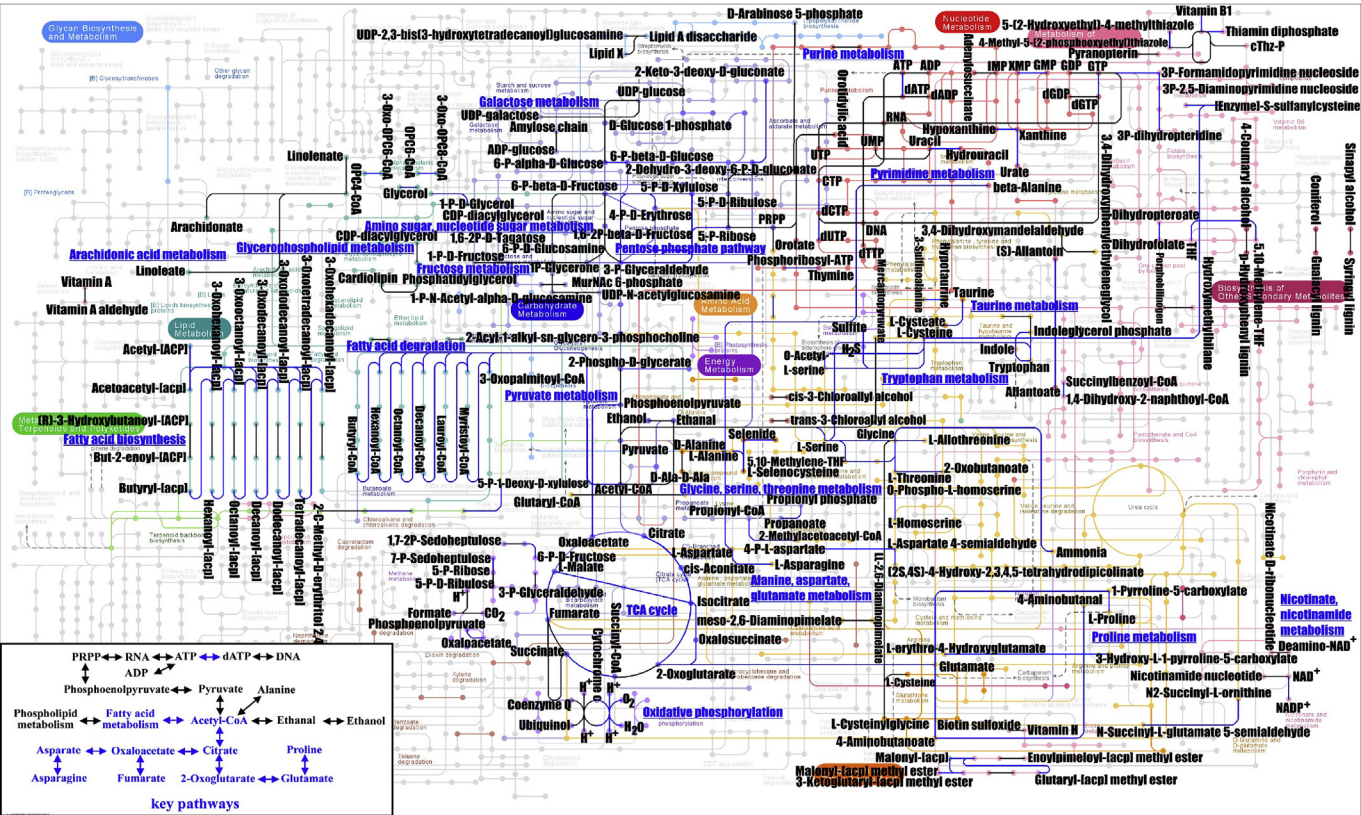| Name	Product A	Product B	Relative intensity variations of TCEP organic intermediates
Proposed structure			
Molecular formula	$C_4H_9Cl_2O_4P$	$C_6H_{13}Cl_2O_5P$	
$[M+H]^+$: theoretical m/z	222.9688	266.9950	
$[M+H]^+$: observed m/z	222.9689	266.9951	
Retention time (min)	2.79	3.34	
Extracted ion chromatography			
Name	Product C		Relative abundance variations of TCEP organic intermediates
Proposed structure			
Molecular formula	$C_2H_6ClO_4P$		
$[M+H]^+$: theoretical m/z	160.9768		
$[M+H]^+$: observed m/z	160.9772		
Retention time (min)	2.53		
Extracted ion chromatography			

Fig. 4. The metabolism network related to the different regulated expression proteins in cells exposed to 20 min degrading product mixture.
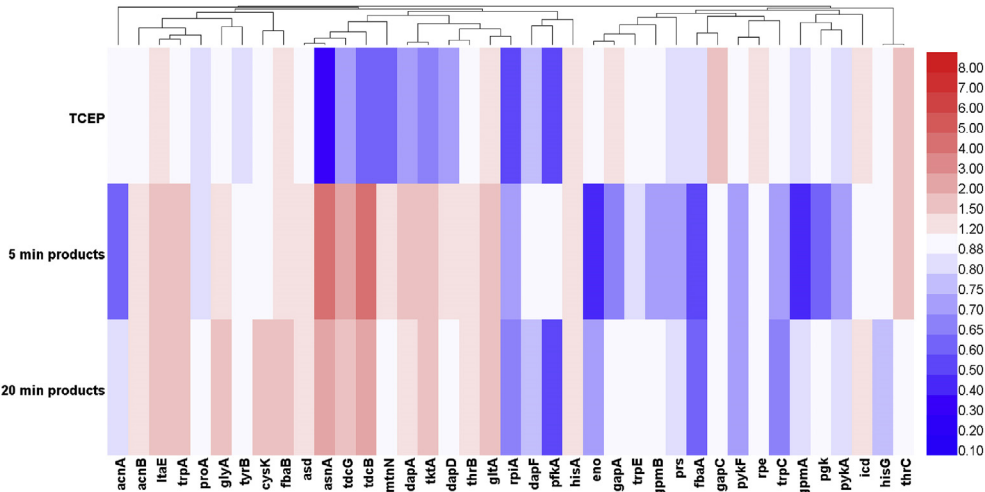

Fig. 5. Different regulated expression proteins related to biosynthesis of amino acids.

Table 2 shows the EE/O result. The EE/O value in the 254 nm UV + 44.0 μM H_2O_2 system was 0.033 kWh m^{-3} order^{-1}. For the influence factor experiments, EE/O values increased when k_{obs} decreased. When the concentration of H_2O_2 increased from 4.4 μM to 220.0 μM, EE/O presented a rising trend (from 0.028 kWh m^{-3} order^{-1} to 0.116 kWh m^{-3} order^{-1}), indicating that excessive H_2O_2 addition increased the energy consumption. Therefore, the addition of H_2O_2 should be properly controlled. Concerning the effect of pH, EE/O remained in the range in the range of 0.031–0.033 kWh m^{-3} order^{-1} under neutral and acidic conditions. Strong alkaline

conditions induced an important increase of EE/O to 0.063 kWh m^{-3} order^{-1}. For HA, EE/O increased from 0.033 kWh m^{-3} order^{-1} to 0.080 kWh m^{-3} order^{-1} as the HA concentration increased. Nitrate had a slight effect on EE/O. These results indicate that the experimental conditions should be maintained in neutral or acidic pH, and the removal of HA by pretreatment would be conducive to TCEP removal. For an actual UV/H_2O_2 treatment process, the assessment of overall cost should take account of electrical cost, chemical reagent cost (e.g., H_2O_2 addition), etc.

Table 2
EE/O values for TCEP degradation in UVH$_2$O$_2$ system.

Reaction	P (kW)	k_{obs} (h)	t (h)	Pt (kWh)	V (m^3)	EE/O
220.0 μM H$_2$O$_2$	7.9×10^{-4}	0.0437	0.88	6.95×10^{-4}	1.0×10^{-4}	0.1158
88.0 μM H$_2$O$_2$	7.9×10^{-4}	0.1015	0.38	2.99×10^{-4}	1.0×10^{-4}	0.0498
44.0 μM H$_2$O$_2$	7.9×10^{-4}	0.1548	0.25	1.96×10^{-4}	1.0×10^{-4}	0.0327
22.0 μM H$_2$O$_2$	7.9×10^{-4}	0.1851	0.21	1.64×10^{-4}	1.0×10^{-4}	0.0273
8.8 μM H$_2$O$_2$	7.9×10^{-4}	0.1795	0.21	1.69×10^{-4}	1.0×10^{-4}	0.0282
4.4 μM H$_2$O$_2$	7.9×10^{-4}	0.1828	0.21	1.66×10^{-4}	1.0×10^{-4}	0.0277
pH = 3.0	7.9×10^{-4}	0.1596	0.24	1.90×10^{-4}	1.0×10^{-4}	0.0317
pH = 5.0	7.9×10^{-4}	0.1655	0.23	1.83×10^{-4}	1.0×10^{-4}	0.0306
pH = 7.0	7.9×10^{-4}	0.1548	0.25	1.96×10^{-4}	1.0×10^{-4}	0.0327
pH = 9.0	7.9×10^{-4}	0.1563	0.25	1.94×10^{-4}	1.0×10^{-4}	0.0324
pH = 11.0	7.9×10^{-4}	0.0798	0.48	3.80×10^{-4}	1.0×10^{-4}	0.0634
Humic acid	7.9×10^{-4}	0.0630	0.61	4.82×10^{-4}	1.0×10^{-4}	0.0803
NO$_3^-$	7.9×10^{-4}	0.1591	0.24	1.91×10^{-4}	1.0×10^{-4}	0.0318

● EE/O has the unit of kWh m^{-3} order^{-1}; P represents the total electrical power to drive UV irradiation entering the matrix, kW; t indicates the time which 90% of targeted contaminant is degraded, h; V is the volume of reaction matrix, m^3.
● The dosages of humic acid and NO$_3^-$ are 100 mg L^{-1}.

4. Conclusion

The degradation of TCEP using UV/H$_2$O$_2$ followed a pseudo-first order reaction with a k_{obs} of 0.155 min^{-1}, and ·OH was confirmed to be the dominating active radical species. As the reaction proceeded, TCEP was transformed to several hydroxylated and dechlorinated products. The significant activation of critical metabolism pathways in *E. coli* cells exposed to degradation intermediate mixture suggested that the toxicity of these degradation products was obviously weakened. In conclusion, the hydroxylation and dechlorination of TCEP by UV/H$_2$O$_2$ was effective for its detoxification.

Acknowledgement

Appendix A. Supplementary data

Supplementary data related to this article can be found at https://doi.org/10.1016/j.chemosphere.2017.09.111.

References

Andresen, J.A., Grundmann, A., Bester, K., 2004. Organophosphorus flame retardants and plasticisers in surface waters. Sci. Total Environ. 332, 155–166.

Araki, A., Saito, I., Kanazawa, A., Morimoto, K., Nakayama, K., Shibata, E., Tanaka, M., Takigawa, T., Yoshimura, T., Chikara, H., 2014. Phosphorus flame retardants in indoor dust and their relation to asthma and allergies of inhabitants. Indoor Air 24, 3–15.

Buxton, G.V., 1988. Critical Review of rate constants for reactions of hydrated electrons, hydrogen atoms and hydroxyl radicals (•OH/•O$^-$) in aqueous solution. J. Phys. Chem. Ref. Data 17, 513–886.

Canonica, S., Jans, U., Stemmler, K., Hoigne, J., 1995. Transformation kinetics of phenols in water: photosensitization by dissolved natural organic material and aromatic ketones. Environ. Sci. Technol. 29, 1822–1831.

Cristale, J., Hurtado, A., Gomez-Canela, C., Lacorte, S., 2016. Occurrence and sources of brominated and organophosphorus flame retardants in dust from different indoor environments in Barcelona, Spain. Environ. Res. 149, 66–76.

Crittenden, J.C., Hu, S., Hand, D.W., Green, S.A., 1999. A kinetic model for H$_2$O$_2$/UV process in a completely mixed batch reactor. Water Res. 33, 2315–2328.

Dodd, M.C., Kohler, H.-P.E., Von Gunten, U., 2009. Oxidation of antibacterial compounds by ozone and hydroxyl radical: elimination of biological activity during aqueous ozonation processes. Environ. Sci. Technol. 43, 2498–2504.

Ezechias, M., Covino, S., Cajthaml, T., 2014. Ecotoxicity and biodegradability of new brominated flame retardants: a review. Ecotoxicol. Environ. Saf. 110, 153–167.

Ghaly, M.Y., Härtel, G., Mayer, R., Haseneder, R., 2001. Photochemical oxidation of p-chlorophenol by UV/H$_2$O$_2$ and photo-Fenton process. A comparative study. Waste Manag. 21, 41–47.

Guo, J.H., Venier, M., Salamova, A., Hites, R.A., 2017. Bioaccumulation of Dechloranes, organophosphate esters, and other flame retardants in Great Lakes fish. Sci. Total Environ. 583, 1–9.

He, X., Cruz, A.A.D.L., Dionysiou, D.D., 2013. Destruction of cyanobacterial toxin cylindrospermopsin by hydroxyl radicals and sulfate radicals using UV-254 nm activation of hydrogen peroxide, persulfate and peroxymonosulfate. J. Photochem. Photobiol. A Chem. 251, 160–166.

Huber, M.M., Canonica, S., Park, G.Y., Von Gunten, U., 2003. Oxidation of pharmaceuticals during ozonation and advanced oxidation processes. Environ. Sci. Technol. 37, 1016–1024.

Keen, O.S., Linden, K.G., 2013. Degradation of antibiotic activity during UV/H2O2 advanced oxidation and photolysis in wastewater effluent. Environ. Sci. Technol. 47, 13020–13030.

Kim, J.W., Isobe, T., Chang, K.H., Amano, A., Maneja, R.H., Zamora, P.B., Siringan, F.P., Tanabe, S., 2011. Levels and distribution of organophosphorus flame retardants and plasticizers in fishes from Manila Bay, the Philippines. Environ. Pollut. 159, 3653–3659.

Kim, S., Jung, J., Lee, I., Jung, D., Youn, H., Choi, K., 2015. Thyroid disruption by triphenyl phosphate, an organophosphate flame retardant, in zebrafish (Danio rerio) embryos/larvae, and in GH3 and FRTL-5 cell lines. Aquat. Toxicol. 160, 188–196.

Kusnadi, E.P., Hannan, K.M., Hicks, R.J., Hannan, R.D., Pearson, R.B., Kang, J., 2015. Regulation of rDNA transcription in response to growth factors, nutrients and energy. Gene 556, 27–34.

Martinez-Carballo, E., Gonzalez-Barreiro, C., Sitka, A., Scharf, S., Gans, O., 2007. Determination of selected organophosphate esters in the aquatic environment of Austria. Sci. Total Environ. 388, 290–299.

Meeker, J.D., Stapleton, H.M., 2010. House dust concentrations of organophosphate flame retardants in relation to hormone levels and semen quality parameters. Environ. Health Perspect. 118, 318–323.

Meng, N.C., Bo, J., Chow, C.W.K., Saint, C., 2010. Recent developments in photocatalytic water treatment technology: a review. Water Res. 44, 2997–3027.

Meyer, J., Bester, K., 2004. Organophosphate flame retardants and plasticisers in wastewater treatment plants. J. Environ. Monit. 6, 599–605.

Munoz, M.J., Moreno, N.N., Giono, L.E., Botto, A.E.C., Dujardin, G., Bastianello, G., Lavore, S., Torres-Mendez, A., Menck, C.F.M., Blencowe, B.J., Irimia, M., Foiani, M., Komblihtt, A.R., 2017. Major roles for pyrimidine dimers, nucleotide excision repair, and ATR in the alternative splicing response to UV irradiation. Cell Rep. 18, 2868–2879.

Ou, H.S., Liu, J., Ye, J.S., Wang, L.L., Gao, N.Y., Ke, J., 2017. Degradation of tris(2-chloroethyl) phosphate by ultraviolet-persulfate: kinetics, pathway and intermediate impact on proteome of *Escherichia coli*. Chem. Eng. J. 308, 386–395.

Pillai, S.C., Stangar, U.L., Byrne, J.A., Perez-Larios, A., Dionysiou, D.D., 2015. Photocatalysis for disinfection and removal of contaminants of emerging concern. Chem. Eng. J. 261, 1–2.

Reemtsma, T., Weiss, S., Mueller, J., Petrovic, M., Gonzalez, S., Barcelo, D., Ventura, F., Knepper, T.P., 2006. Polar pollutants entry into the water cycle by municipal wastewater: a European perspective. Environ. Sci. Technol. 40, 5451–5458.

Ruan, X.C., Ai, R., Jin, X., Zeng, Q.F., Yang, Z.Y., 2013. Photodegradation of tri(2-chloroethyl) phosphate in aqueous solution by UV/H$_2$O$_2$. Water, Air, & Soil Pollut. 224, 1–10.

Shen, Y.S., Wang, D.K., 2002. Development of photoreactor design equation for the treatment of dye wastewater by UV/H$_2$O$_2$ process. J. Hazard. Mater. 89, 267–277.

Shi, Y.L., Gao, L.H., Li, W.H., Wang, Y., Liu, J.M., Cai, Y.Q., 2016. Occurrence, distribution and seasonal variation of organophosphate flame retardants and plasticizers in urban surface water in Beijing, China. Environ. Pollut. 209, 1–10.

Stackelberg, P.E., Furlong, E.T., Meyer, M.T., Zaugg, S.D., Henderson, A.K., Reissman, D.B., 2004. Persistence of pharmaceutical compounds and other organic wastewater contaminants in a conventional drinking-water-treatment plant. Sci. Total Environ. 329, 99–113.

Ta, N., Li, C., Fang, Y., Liu, H., Lin, B., Jin, H., Tian, L., Zhang, H., Zhang, W., Xi, Z., 2014. Toxicity of TDCPP and TCEP on PC12 cell: changes in CAMKII, GAP43, tubulin and NF-H gene and protein levels. Toxicol. Lett. 227, 164–171.

Waaijers, S.L., Hartmann, J., Soeter, A.M., Helmus, R., Kools, S.A., de Voogt, P., Admiraal, W., Parsons, J.R., Kraak, M.H., 2013. Toxicity of new generation flame retardants to *Daphnia magna*. Sci. Total Environ. 463, 1042–1048.

Watts, M.J., Linden, K.G., 2008. Photooxidation and subsequent biodegradability of recalcitrant tri-alkyl phosphates TCEP and TBP in water. Water Res. 42, 4949–4954.

Yuan, X., Lacorte, S., Cristale, J., Dantas, R.F., Sans, C., Esplugas, S., Qiang, Z., 2015. Removal of organophosphate esters from municipal secondary effluent by ozone and UV/H$_2$O$_2$ treatments. Sep. Purif. Technol. 156, 1028–1034.

Zeng, X.Y., Liu, Z.Y., He, L.X., Cao, S.X., Song, H., Yu, Z.Q., Sheng, G.Y., Fu, J.M., 2015. The occurrence and removal of organophosphate ester flame retardants/plasticizers in a municipal wastewater treatment plant in the Pearl River Delta, China. J. Environ. Sci. Health Part A Toxic Hazard. Subst. Environ. Eng. 50, 1291–1297.

Zhou, H., Smith, D.W., 2001. Advanced technologies in water and wastewater treatment. Can. J. Civ. Eng. 28, 49–66.